

 Open access • Journal Article • DOI:10.1002/BEM.21793

Personal distributed exposimeter for radio frequency exposure assessment in real environments. — Source link

Arno Thielens, Hans De Clercq, Sam Agneessens, Jeroen Lecoutere ...+8 more authors

Institutions: Ghent University, Catholic University of Leuven

Published on: 01 Oct 2013 - Bioelectromagnetics (Bioelectromagnetics)

Topics: Anechoic chamber

Related papers:

- [Guidelines for limiting exposure to time-varying electric, magnetic, and electromagnetic fields \(up to 300 GHz\)](#)
- [Factors influencing uncertainty in measurement of electric fields close to the body in personal RF dosimetry.](#)
- [The association between exposure determined by radiofrequency personal exposimeters and human exposure: a simulation study.](#)
- [Calibration and uncertainties in personal exposure measurements of radiofrequency electromagnetic fields.](#)
- [Statistical analysis of personal radiofrequency electromagnetic field measurements with nondetects](#)

Share this paper:    

View more about this paper here: <https://typeset.io/papers/personal-distributed-exposimeter-for-radio-frequency-bjidppug4m>

Distributed On Person Exposimeters for Radio Frequency Exposure Assessment in Real Environments

**Arno, Thielens¹, Hans, De Clercq², Sam, Agneessens³, Jeroen, Lecoutere², Leen, Verloock¹,
Frederick, Declercq³, Günter, Vermeeren¹, Emmeric, Tanghe¹, Hendrik Rogier³, Robert, Puers²,
Luc, Martens¹, and Wout, Joseph¹**

(email: arno.thielens@intec.UGent.be, tel: +32 9 33 14918, fax: +32 9 33 14899)

**¹ Wireless & Cable Group, Department of Information Technology, Ghent University / iMinds
Ghent, Belgium**

**² Microelectronics and Sensors Group, Department of Electrotechnical Engineering, Catholic
University Leuven
Heverlee, Belgium**

**³ Electromagnetics Group, Department of Information Technology, Ghent University
Ghent, Belgium**

Running title- **Personal Distributed Exposimeter**

Grant Sponsor- This research was funded by the Research Foundation – Flanders (FWO-V)
under grant agreement No 3G004612.

Abstract- For the first time, a personal distributed exposimeter (PDE) for radio frequency (RF) measurements is presented. This PDE is designed based on numerical simulations and experimentally evaluated using textile antennas and wearable electronics. A prototype of the PDE is calibrated in an anechoic chamber. Compared to conventional exposimeters, which only measure in 1 position on the body, an excellent isotropy of 0.5 dB (a factor of 1.1) and a 95% confidence interval of 7 dB (a factor of 5) on measured power (densities) are measured.

Key Words- **Dosimetry; Radio frequency exposure; Textile antennas; PIFA; Wearable electronics**

Assessing the typical range of exposures to radio frequency (RF) radiation is important to study compliance with international guidelines, such as ICNIRP [ICNIRP, 1998], and national legislation. Moreover, it is also crucial for environmental safety and epidemiological studies, quantifying potential health effects of RF radiation. The personal, daily electromagnetic field exposure of a subject is usually assessed by means of exposimeters or personal dosimeters, for which a protocol has been developed [Röösli et al., 2010]. The currently existing exposimeters are frequently used in measurement campaigns of exposures to RF radiation [Neubauer et al., 2007; Joseph et al., 2008b, 2010; Knafel et al., 2008; Röösli et al., 2008; Frei et al., 2009; Viel et al., 2009; Bolte and Eikelboom, 2012]. However, they are faced with very large uncertainties due to shadowing of the body and variability of their position on the body [Blas et al., 2007; Bahillo et al., 2008; Neubauer et al., 2010; Iskra et al., 2010, 2011; Bolte et al., 2011]. RF electromagnetic fields are incident on the human body and will be reflected and absorbed. This causes the electric field (strength) at the position of an exposimeter to be different from the incident electric field (strength). This reflection and absorption will be

dependent on the subject's morphology [Kühn et al., 2009; Neubauer et al., 2009, 2010; Bakker et al., 2010; El Habachi et al., 2010]. Consequently an exposimeter will measure the total electric fields (i.e., including scattering of the body) instead of the incident fields, which are necessary for quantification and comparison of exposure levels [ICNIRP, 1998]. Current exposimeters also show an unwanted dependence on the polarization of the incident electric fields [Bolte et al., 2011]. Other uncertainties of the current exposimeters are out-of-band detections, a possible non-linear power response, and technical defects that may occur [Bolte et al., 2011].

For the first time, an on-body worn personal distributed exposimeter (PDE) containing multiple RF acquisition nodes is proposed. The nodes are optimally distributed on the body and carefully calibrated in an anechoic chamber using a real human subject. In addition, numerical simulations of a heterogeneous human body phantom in realistic electromagnetic environments are carried out in order to determine an optimal placement of the nodes for measurement of the incident electric fields. This PDE is demonstrated at 950 MHz, the Global System for Mobile Communications (GSM) downlink frequency which is present in most environments [Joseph et al., 2010] and for which the incident fields can be described using stochastic parameters [Vermeeren et al. 2008; Iskra et al., 2011]. A further novelty of this exposimeter is the use of textile antennas, which are lightweight, flexible, and have comparable performance to their rigid counterparts [Locher et al., 2006; Hertleer et al., 2007, Agneessens et al., 2012] and wearable electronics [Carta et al., 2009; Jourand et al., 2010], which can both be unobtrusively integrated in clothing in order to maximize wearability of the PDE [Reusens et al., 2009].

The antenna chosen for this application is a quarter wavelength planar inverted F antenna (PIFA) that offers a good trade-off between antenna performance and size [Declercq et al., 2011]. The antenna is constructed entirely from lightweight, flexible and breathable materials, in order to maximize wearability. Furthermore, the conductive ground plane, inherent to the antenna topology, minimizes the influence of the body on the antenna performance. The antenna covers the GSM 950 MHz downlink frequency band and has a 60 MHz bandwidth. The simulated gain and beam width at half maximum are 2.9 dBi and 110° respectively, while the antenna efficiency is 76.6%.

Each textile antenna is connected to an RF-exposure acquisition system. These nodes contain a commercially available receiver that is tuned for a 950 MHz link (CC1100E, Texas Instruments, Dallas, TX, USA) and a microcontroller (PIC18f14k22, Microchip, Chandler, AZ, USA) for data management. In this first prototype, the RF-exposure data is communicated via I2C to a main unit that interfaces with a personal computer using USB. The architecture is made modular, such that the amount of nodes is easily extendable and other frequency bands can be explored. Acquisition parameters, such as sample rate and frequency channel can be adjusted during measurements. Since the used antennas, the acquisition nodes, and all interconnections are all flexible and lightweight, these can be comfortably worn by volunteers without impeding body movement.

The design of the distributed exposimeter is based on finite-difference time-domain (FDTD) simulations using the Virtual Family Male (VFM) [Christ et al., 2010] (grid step = 1.5 mm) in upright anatomical position. This is a heterogeneous human body model consisting of 81 different tissues, based upon magnetic resonance imaging of a healthy volunteer with a BMI (body mass index) of 22.3 kg/m². The dielectric properties assigned to the phantom's tissues

are taken from the Gabriel database [Gabriel et al., 1996]. The electric fields surrounding the phantom can be determined by means of FDTD simulations and using the methods presented in Vermeeren et al. [2008, 2012] and Iskra et al. [2011], enables the determination of these fields for realistic environments.

To model the PDE, potential positions to deploy the wearable antennas (measurement positions) are determined at 1 cm from the phantom's upper body. In addition the required number of antennas (N) for a PDE is determined. In the procedure it is taken into account that realistic antennas have a finite surface and may not overlap. In cylindrical coordinates (see Fig. 1 (a)) a discretization step in the z-coordinate (along the body's main axis) of 10 cm is chosen. For the azimuth angle $\varphi = 0: \Delta\varphi: 2\pi$ a step of $\Delta\varphi = \pi/6$ is chosen. Furthermore antennas may not be positioned on the phantom's face.

A linear regression model based upon the simulation results is constructed. This enables us to determine the incident root-mean-squared (RMS) electric fields E_{RMS}^{free} , using the electric fields recorded by the PDE $E_{RMS,i}^{body}$, with i the i^{th} selected measurement position. The model is described by the following equation:

$$E_{RMS}^{free} = b_0 + \sum_{i=1}^N b_i E_{RMS,i}^{body} + err \quad (1)$$

with b_i ($i=0..N$) the regression coefficients and err the residual. This regression model was built for the ideal case of 'perfect' sensors that can record the actual $E_{RMS,i}^{body}$ value in position i and for the realistic case of linearly polarized antennas that only record one component in the plane tangential to the body, which is the case for the textile antennas used throughout this paper. We have constructed a step-wise algorithm that selects a set of measurement positions

(and polarizations), minimizing the error-on-prediction for a given posture of a selected phantom.

Figure 1 shows the results of our step-wise algorithm using 4000 observations and 1000 control values in the (realistic) Indoor Pico-cell environment [Vermeeren et al., 2008; Iskra et al., 2011]. The error-on-prediction of the linear regression model in (1) is shown in Figure 1 (b) as a function of the number of measurement positions. Both perfect sensors and linearly polarized textile antennas are considered. The allowed orientations of the linearly polarized antennas in the tangent plane to the body are multiples of $\pi/9$. Some accuracy is lost (1.7% on average) when only one component of the field can be measured, compared to a perfect measurement of the full root RMS values. Using a resolution of 20° ($\pi/9$) we can estimate the incident electric fields with an average error of 13% using 3 measurement positions (i.e., 3 antennas on the body) and 9.2% using 10 measurement positions. We thus prove that it is possible to accurately predict the incident electric fields using only a few measurement positions on the body. Figure 1 (a) shows the 3 positions (blue ellipses) that, when combined, have the lowest error-on-prediction found by the model. The (approximate) polarization is shown by black arrows and a possible location for the processing unit is shown in red.

Using a set of 3 textile antennas placed on the positions predicted by the step-wise algorithm (Fig. 1 (a)), a first prototype of the exposimeter is constructed. This model is calibrated in an anechoic chamber on a human subject with a BMI comparable to that of the VFM ($\pm 1 \text{ kg/m}^2$). The subject is placed in an anechoic chamber in the far field of a dipole radiating at 950 MHz in an upright anatomical position and is rotated over 360° in azimuth angle ϕ and this for two orthogonal polarizations (horizontal and vertical, which are perpendicular and parallel to the

subject's axis of rotation, respectively) of the dipole which emits at a constant output power. The subject is rotated in ϕ because in reality the azimuthal angle of incidence of a measured incident plane wave is unknown. Each antenna (i) will receive a certain power $P_{r,i}^{body}$ as a function of ϕ . To determine an average measured response R_{meas} (dB), these received powers are averaged over ϕ and divided by the received power of the antennas in free-space P_r^{free} , averaged over the subject's rotation axis [CENELEC, 2008]:

$$R_{meas} = 10 \times \log \left(\frac{\langle \frac{1}{N} \sum_{i=1}^N P_{r,i}^{body} \rangle_{\phi}}{P_r^{free}} \right) \quad (2)$$

An average of the received powers of different antennas is made in a PDE; this reduces the variance on the measured data. Figure 2 shows the response R_{meas} corresponding to the lowest 95% confidence interval (c_{95}) as a function of the number of antennas in the PDE (1 antenna corresponds with a single exposimeter). For the horizontal polarization a 6.5 dB reduction (division by a factor of 4.5) in c_{95} for 3 antennas is measured on an initial c_{95} of 13.5 dB (a factor of 22.4) for the best measurement with 1 textile antenna (a single exposimeter). A 5 dB reduction (division by a factor of 3) on 12.4 dB (a factor of 17.4) is measured on the c_{95} for the vertically polarized incident plane waves. This results in a final c_{95} of 7 dB (a factor of 5 for horizontal polarization) and 7.4 dB (a factor of 5.5 for vertical polarization).

In a previous study by Bolte et al. [2011] a commercial, single exposimeter was worn on the right hip by a subject rotated over 360° under exposure by a GSM downlink signal. An interquartile distance of 6.5 dB (a factor of 4.5) and 15.5 dB (a factor of 35) were measured for incident horizontal and vertical polarizations, respectively. In Neubauer et al. [2010] different possible locations of an exposimeter on the human body were investigated on a human body phantom in a simulated multipath environment at 946 MHz. This led to an interquartile

distance of 8 dB (factor of 6) and a c_{90} of 18 dB (factor of 62). Our measurements using 3 antennas show an interquartile distance of 4.5 dB (a factor of 2.8) and the aforementioned c_{95} of 7 dB (factor of 5) and 7.5 dB (factor of 5.5) for a horizontally and vertically polarized source, which are considerably better. A c_{95} of 18.5 dB (a factor of 70.8) on the body is estimated for commercial exposimeters at 900 MHz in realistic environments [Iskra et al., 2011]. The FDTD simulations at 950 MHz show a c_{95} of 25 dB (a factor of 316) on the VFM for a single dosimeter in the same exposure conditions as the calibration and 22 dB (a factor of 158) in realistic exposure conditions. All these values are much larger than the c_{95} 's measured in this study.

The measurements show that a huge improvement in variance and thus accuracy can be obtained using just 3 antennas. Moreover, the PDE also exhibits excellent performance in terms of isotropy (I), defined as the ratio of R_{meas} between 2 orthogonal polarizations. Figure 2 shows that for the combination of the three textile antennas $I = 0.5$ dB (a factor of 1.1), which is much better than the I of 6.4 dB (a factor of 4.4) for commercial exposimeters located on the body [Bolte et al., 2011]. The important quantity for exposure assessment is the ratio R of the power densities S:

$$R = 10 \times \log \left(\frac{\left(\frac{1}{N} \sum_{i=1}^N S_i^{body} \right) \lambda \phi}{S^{free}} \right) = R_{meas} + A \quad (4)$$

with S_i^{body} the power density on the location of antenna i , S^{free} the free-space power density and A represents a logarithmic correction factor. Since an R of zero is desired for accurate measurements, A is determined to be 15.4 dB (a factor of 34.7).

In general, one can conclude that a personal distributed exposimeter with a good accuracy can be constructed using a limited number of antennas. We have developed a regression model to

construct such a exposimeter, based on numerical simulations, and have calibrated a preliminary model of the exposimeter, consisting of 1, 2 or 3 antennas, in an anechoic chamber, using a real human. It is shown that the prototype of the PDE performs much better than commercially available exposimeters.

Future research will consist of extending the PDE to other frequencies and calibrating it using multiple subjects. The concept can also be used to distinguish between near-body and far-from-body sources.

ACKNOWLEDGEMENTS

W. Joseph and E. Tanghe are Post-Doctoral Fellows of the FWO-V.

REFERENCES

Agneessens S, Van Torre P, Declercq F, Spinnewyn B, Stockman G, Rogier H, Vande Ginste D. 2012. Design of a Wearable, Low-Cost, Through-Wall Doppler Radar System. *International Journal of Antennas and Propagation*, vol. 2012, Article ID 840924, 9 pages, 2012. doi:10.1155/2012/840924.

Bahillo A, Blas J, Fernández P, Lorenzo RM, Mazuelas S, Abril EJ. E-field assessment errors associated with RF dosimeters for different angles of arrival. 2008. *Radiat Prot Dosimetry* 132(1): 51-56.

Bakker J F, Paulides M M, Christ A, Kuster N, van Rhooon G C. 2010. Assessment of induced SAR in children exposed to electromagnetic plane waves between 10 MHz and 5.6 GHz. *Phys Med Biol* 55(11): 3115-30.

Blas J, Lago FA, Fernández P, Lorenzo RM, Abril EJ. 2007. Potential exposure assessment errors associated with body-worn RF dosimeters. 2007. *Bioelectromagnetics* 28: 573-576.

Bolte J.F.B., Van der Zande G., Kamer J., 2011. Calibration and uncertainties in personal exposure measurements of radiofrequency electromagnetic fields. *Bioelectromagnetics* 32(8): 652-663.

Bolte JFB, Eikelboom T. 2012. Personal radiofrequency electromagnetic field measurements in the Netherlands: Exposure level and variability for everyday activities, times of day and types of area. *Environment International* 48: 133-142.

Carta R, Jourand P, Hermans B, Thone J, Brosteaux D, Vervust T, Bossuyt F, Axisa F, Vanfleteren J, Puers R. 2009. Design and implementation of advanced systems in a flexible-stretchable technology for biomedical applications. *Sensors and Actuators A, Physical* 156 (1): 79-87.

European Committee for Electrotechnical Standardization (CENELEC). 2008. Basic standard for the in-situ measurement of electromagnetic field strength related to human exposure in the vicinity of base stations. Brussel, Belgium. EN 50492:2008

Christ A, Kainz W, Hahn E G, Honegger K, Zefferer M, Neufeld E, Rascher W, Janka R, Bautz W, Chen J, Kiefer B, Schmitt P, Hollenbach H, Shen J, Oberle M, Szczerba D, Kam A, Guag J W, Kuster N. 2010. The Virtual Family, development of surface-based anatomical models of two adults and two children for dosimetric simulations. *Phys Med Biol* 55: N23-38.

Declercq F, Georgiadis A, Rogier H. 2011. Wearable aperture-coupled shorted solar patch antenna for remote tracking and monitoring applications. *Proceedings of the 5th European Conference on Antennas and Propagation (EUCAP)*.

El Habachi A, Conil E, Hadjem A, Vazquez E, Wong MF, Gati A, Fleury G, Wiart J. 2010. Statistical analysis of whole-body absorption depending on anatomical human characteristics at a frequency of 2.1 GHz. *Phys Med Biol* 55: 1875-1887.

Frei P, Mohler E, Neubauer G, Theis G, Burgi A, Frohlich J, Braun-Fahrlander C, Bolte J, Egger M, Roösli, M. 2009. Temporal and spatial variability of personal exposure to radiofrequency electromagnetic fields. *Environmental Research* (109):779–785.

Gabriel C, Gabriely S, Corthout E. 1996. The dielectric properties of biological tissues. *Phys Med Biol* 41: 2231-2293.

Hertleer C, Tronquo A, Rogier H, Vallozzi L, Van Langenhove L. 2007. Aperture-Coupled Patch Antenna for Integration Into Wearable Textile Systems. *IEEE Antennas and Wireless Propagation Letters* 6: 392-395.

International Commission on Non-Ionizing Radiation Protection. 1998. Guidelines for limiting exposure to time-varying electric, magnetic, and electromagnetic fields (up to 300 GHz). *Health Physics* 74: 494-522.

Iskra S, McKenzie R, Cosic I. 2011. Monte Carlo simulations of the electric field close to the body in realistic environments for application in personal radiofrequency dosimetry. *Radiat Prot Dosimetry* 147(4): 517-527.

Iskra S, McKenzie R, Cosic I. 2010. Factors influencing uncertainty in measurement of electric fields close to the body in personal RF dosimetry. *Radiat Prot Dosimetry* 140 (1): 25-33.

Joseph W, Vermeeren G, Verloock L, Heredia MM, Martens L. 2008. Characterization of personal RF electromagnetic field exposure and actual absorption for the general public. *Health Phys* 95(3):317-330.

Joseph W, Vermeeren G, Verloock L, Martens L. 2010. Estimation of whole-body SAR from electromagnetic fields using personal exposure meters. *Bioelectromagnetics* 31(4): 286-295.

Jourand P, De Clercq H, Puers R. 2010. Robust monitoring of vital signs integrated in textile. *Sensors and Actuators A, Physical* 161 (1-2): 288-296.

Knafl U, Lehmann H, and Riederer M. 2008. Electromagnetic field measurements using personal exposimeters. *Bioelectromagnetics* 29:160-162.

Kühn S, Jennings W, Christ A, Kuster N. 2009. Assessment of induced radio-frequency electromagnetic fields in various anatomical human body models. *Phys Med Biol* 54: 875-890.

Locher I, Klemm M, Kirstein T, Troster G. 2006. Design and Characterization of Purely Textile Patch Antennas. *IEEE Transactions on Advanced Packaging* 29: 777-788.

Neubauer G, Feychting M, Hamnerius Y, Kheifets L, Kuster N, Ruiz I, Schüz J, Uberbacher R, Wiart J, Rösli M. 2007. Feasibility of future epidemiological studies on possible health effects of mobile phone base stations. *Bioelectromagnetics* 28:224-230.

Neubauer G, Preiner P, Cecil S, Mitrevski N, Gorter J, Garn H. 2009. The relation between the specific absorption rate and electromagnetic field intensity for heterogeneous exposure conditions at mobile communications frequencies. 2009. *Bioelectromagnetics* 30: 651-662.

Neubauer G, Cecil S, Giczi W, Petric B, Preiner P, Fröhlich J, Rösli M. 2010. The association between exposure determined by radiofrequency personal exposimeters and

human exposure: a simulation study. *Bioelectromagnetics* 31: 535-545.

Reusens E, Joseph W, Latré B, Braem B, Vermeeren G, Tanghe E, Martens L, Blondia C,

Moerman I. 2009. Characterization of On-Body Communication Channel and Energy

Efficient Topology Design for Wireless Body Area Networks. *IEEE Transactions on*

Information Technology in Biomedicine 13 (6): 933-945.

Roelens L, Joseph W, Reussens E, Vermeeren G, Martens L. 2008. Characterization of

Scattering Parameters near a Flat Phantom for Wireless Body Area Networks. *IEEE Trans*

Electromag Compat 50 (1): 185 – 193.

Röösli M, Frei P, Mohler E, Braun-Fahrländer C, Burgi A, Fröhlich J, Neubauer G, Theis G,

Egger M. 2008. Statistical analysis of personal radiofrequency electromagnetic field

measurements with nondetects. *Bioelectromagnetics* 29(6):471-478.

Röösli M, Frei P, Bolte J, Neubauer G, Cardis E, Feychting M, Gasjek P, Heinrich S, Joseph

W, Mann S, Martens L, Mohler E, Parslow RC, Poulsen AH, Radon K, Schüz J, Thuroczy G,

Viel J, Vrijheid M. 2010. Conduct of a personal radiofrequency electromagnetic field

measurement study: proposed study protocol. *Environmental Health* 2010, 9-23.

Vermeeren G, Joseph W, Olivier C, Martens L. 2008. Statistical multipath exposure of a human in a realistic electromagnetic environment, *Health Physics* 94: 345 – 54.

Vermeeren G, Joseph W, Martens L. 2012. Statistical multi-path exposure method for assessing the whole-body SAR in a heterogeneous human body model in a realistic environment, accepted in *Bioelectromagnetics*, 18th November 2012.

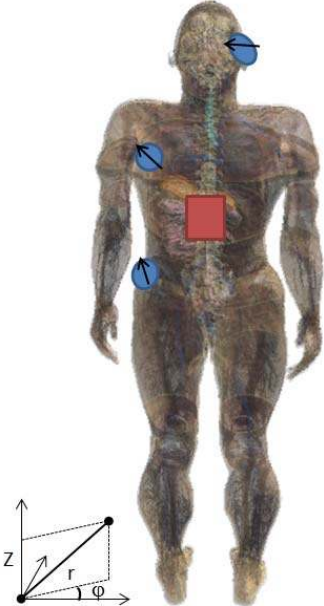
Viel JF, Cardis E, Moissonnier M, deSeze R, Hours M. 2009. Radiofrequency exposure in the French general population: Band, time, location and activity variability. *Environ Int* 35 (8): 1150-1154.

List of captions

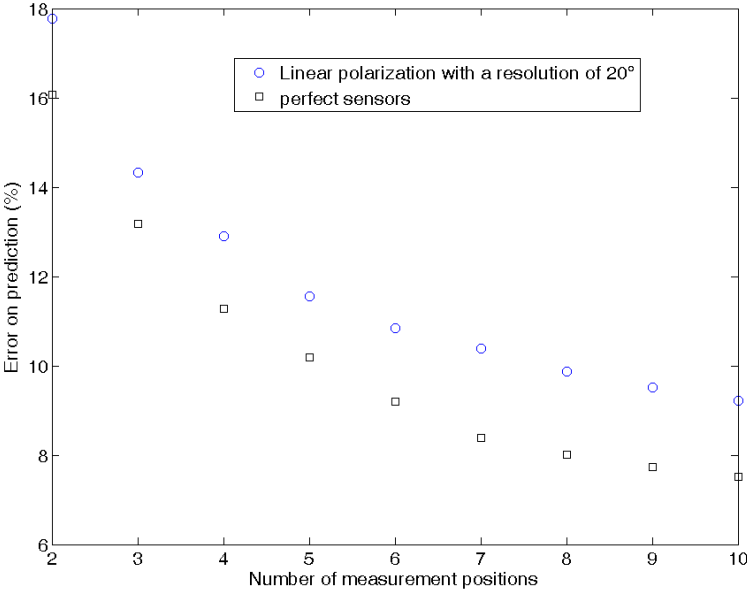
Figure 1: Positions, linear polarizations and error-on-prediction of a personal distributed exposimeter. (a) Optimal positions determined by the step-wise algorithm (indicated by blue ellipses), possible location of the central processing unit (red rectangle), and linear polarizations (black arrows) of the textile antennas at 1cm of the VFM. (b) Average error-on-prediction of the distributed personal exposimeter as a function of the number of measurement positions (number of on-the-body antennas) for 4000 observations and 1000 control values. The errors are given for perfect sensors and for linearly polarized textile antennas at 1cm from the phantom. The resolution of the antennas' linear polarization is 20°.

Figure 2: Angular averaged response R_{meas} with smallest 95% confidence interval as a function of the number of combined antennas on a human subject. The 95% confidence intervals are shown as black bars.

Figures



(a)



(b)

Figure 1

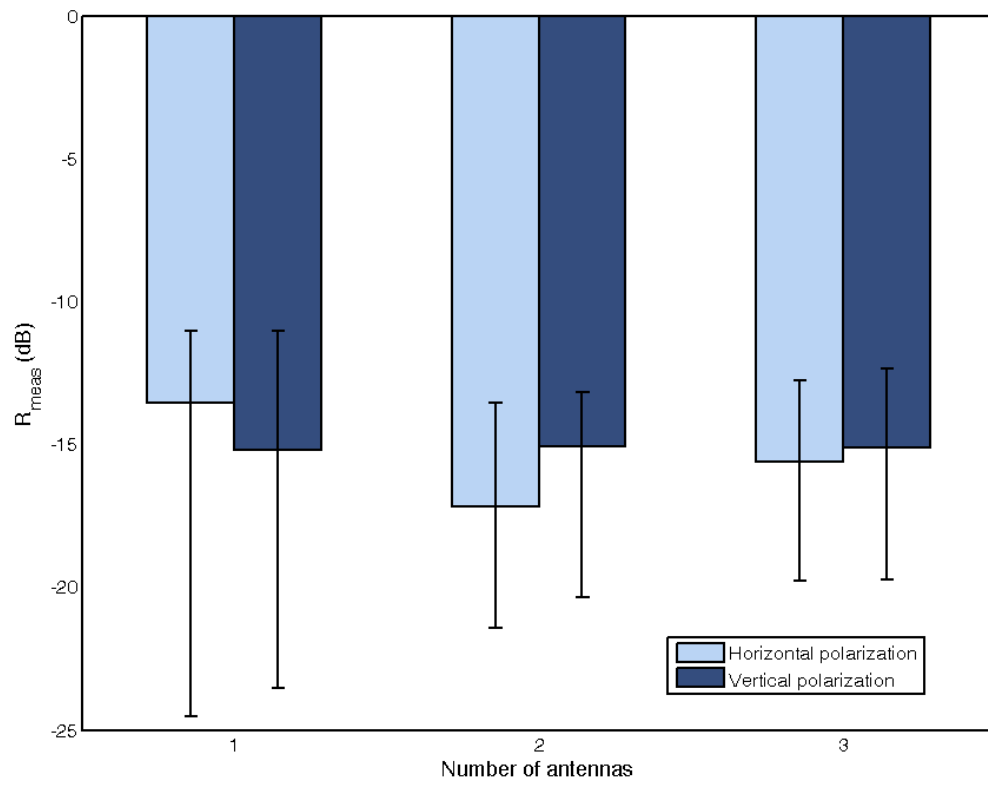


Figure 2